PHYSICAL REVIEW D **80,** 013001 (2009)

kg-mass prototype demonstrator for dual gravitational wave detector: Optomechanical excitation and cooling

M. Anderlini, F. Marino, and F. Marin*

*Dipartimento di Fisica, Università di Firenze, INFN, Sezione di Firenze, and LENS Via Sansone 1, I-50019 Sesto Fiorentino (FI), Italy**

(Received 31 October 2008; published 2 July 2009)

The next generation of gravitational wave (gw) detectors is expected to fully enter into the quantum regime of force and displacement detection. With this aim, it is important to scale up the experiments on opto-mechanical effects from the microscopic regime to large mass systems and test the schemes that should be applied to reach the quantum regime of detection. In this work we present the experimental characterization of a prototype of massive gw detector, composed of two oscillators with a mass of the order of the kg, whose distance is read by a high finesse optical cavity. The mechanical response function is measured by exciting the oscillators through modulated radiation pressure. We demonstrate two effects crucial for the next generation of massive, cryogenic gw detectors (DUAL detectors): (a) the reduction of the contribution of 'local' susceptibility thanks to an average over a large interrogation area. Such effect is measured on the photo-thermal response thanks to the first implementation of a folded-Fabry-Perot cavity; (b) the 'backaction reduction' due to negative interference between acoustic modes. Moreover, we obtain the active cooling of an oscillation mode through radiation pressure, on the described mechanical device which is several orders of magnitude heavier than previously demonstrated radiation-pressure cooled systems.

DOI: 10.1103/PhysRevD.80.013001 PACS numbers: 04.80.Nn, 42.50.Wk, 42.79.−e, 95.55.Ym

I. INTRODUCTION

Ground-based gravitational wave detectors are traditionally classified into large baseline interferometers and resonant antennas. Recently, a new class of gw detectors has been proposed, based on huge masses kept at cryogenic temperature and called DUAL detectors [1–6]. At difference from previous massive cryogenic antennas (such as Weber bars), the DUAL system does not aim at reaching the best peak sensitivity in a narrow band around a resonance frequency, but it takes advantage of elastic forces to achieve a useful sensitivity in a wide frequency range. For this purpose, it is no longer equipped with resonant mechanical amplifiers, and it needs a very sensitive readout. The goal is realizing a detector which covers the acoustic frequency region (1–5 kHz).

A DUAL gw detector exploits two oscillation modes of a mechanical system with a readout symmetric with respect to the center of mass. Because of the geometry, the responses to the readout force of the two modes must be summed, while the responses to the tidal force of the gw are subtracted. In the frequency region between the two resonance frequencies, the susceptibilities of the two modes are in antiphase, giving a reduced response to the readout force and an enhanced response to the gw [2,3] ('backaction reduction'). Such behavior has been recently verified and explored experimentally in Ref. [4], where the authors study the mechanical response to radiation pressure of a cm-size plano-convex mirror which is part of a high Finesse optical cavity. The internal modes of the mirror analyzed are in the $\sim 10^6$ Hz frequency and $\sim 10^{-3}$ kg mass range. It is worth pointing out that the 'backaction reduction' mechanism is also the basis for a proposed scheme of quantum nondemolition measurement.

Two further important effects are considered in the design of DUAL: (a) a clever readout geometry allows to be blind to some low-frequency acoustic modes that would bring thermal and back-action noise peaks in the useful frequency range (mode selectivity); (b) a broad interrogation area enables to reduce the effect of 'local' deformations due to thermal motion and readout force, i.e., from a different point of view, the effect of high frequency modes (wide area readout).

Different configurations of DUAL have been proposed and studied: two nested spheres [1], where the relevant modes are the first quadrupolar mode of the inner and outer sphere; two nested cylinders [3], again acting on the first quadrupolar mode of the nested bodies; a single hollow cylinder [5], exploiting its first and second quadrupolar modes; a symmetric set of cylinders [6], where the first DUAL mode is given by the elastic link between them and the second one by their first oscillation mode.

For any configuration, the possibility of an optical readout is extremely useful for its potentiality to reach a detection sensitivity at the standard quantum limit [7], or even surpass it [8]. An optical scheme expressly conceived for the application in a DUAL detector is proposed and studied in Ref. [9]. The idea is 'folding' a Fabry-Perot cavity in order to interrogate a large detector area with a

*Corresponding author: marin@fi.infn.it

beam bouncing several times between the sensing masses, before being reflected back on itself by the end mirror to close the cavity. Such a kind of folded Fabry-Perot (FFP) has never been implemented experimentally.

An interesting possibility for boosting the sensitivity of massive detectors to short bursts is suggested by Vitali *et al.* [10]. They show that, in some conditions, periodic cycles of fast feedback cooling of the sensitive mechanical mode, followed by a measurement period lasting a fraction of the temperature recovery time, brings an improvement of the sensitivity by even an order of magnitude.

Cooling of a mechanical oscillator by means of radiation pressure [11] has been recently demonstrated on micro-resonators using both active techniques ('cold damping') [12,13], with feedback acting on the optical power impinging on the mirror, or passive schemes ('self-cooling'), exploiting the mechanical effect of red-detuned laser radiation [14–17]. The above results were obtained on effective oscillator masses of less than 1 g, and frequencies in the 10^4–10^8 Hz range. A recent work [18] describes the cooling of a gram-size mirror held by a cantilever flexure, with a resonance frequency of ~100 Hz. Here the cantilever damping is obtained through a so-called hybrid scheme, exploiting active feedback on the cavity length which actually modifies the radiation pressure exerted by detuned laser radiation. The cooling effect can be attributed to the optical spring originated by radiation pressure, modified (with an added reactive component) by feedback. A similar hybrid technique is used also by Corbitt *et al.* [19] to cool a suspended ~1 g mirror, with the difference that here the detuning is modified by feedback acting on the laser frequency instead of the cavity length. However, the system explored in Ref. [19] is very peculiar: the optical spring is so strong that it completely determine the oscillation frequency (around ~1 kHz) and the mirror confinement is provided by the optical potential rather than elastic forces.

A completely different cooling technique has been recently applied to the ~1 kHz fundamental mode of the 3 tons aluminum bar of the AURIGA detector [20]. In that work the feedback is electrical and is applied to the capacitor of the mechanical readout. Starting from a cryostat temperature of 4.2 K, the authors obtain a record temperature of 0.17 mK.

Because of the innovative DUAL concept, on the one hand a preliminary experimental study on a small-scale prototype is required. On the other hand, it is important to scale up the experiments on optomechanical effects from the microscopic to the macroscopic range of masses and in the kHz frequencies, and test the schemes that should be applied to reach the quantum regime of detection. In this work we present the experimental characterization of a prototype of DUAL detector, composed of two oscillators with a mass of the order of the kg, whose distance is read by a high finesse optical cavity. The mechanical response function is measured by exciting the oscillators through modulated radiation pressure. We demonstrate two of the above described effects crucial for the DUAL detectors: (a) the reduction of the contribution of 'local' susceptibility due to average over a large interrogation area. Such effect is measured on the photo-thermal response [21,22] thanks to the first implementation of a folded-Fabry-Perot cavity [9]; (b) the 'backaction reduction' due to negative interference between acoustic modes. Moreover, we obtain the active cooling of an oscillation mode through radiation pressure, on our device, which is orders of magnitude heavier than any previously demonstrated radiation-pressure cooled system.

II. EXPERIMENTAL SETUP

The oscillators are made with two 135 mm wide, 30 mm high aluminum masses (test masses), fixed to frames along their short edge by ~mm thick lateral membranes. The first mass is 30 mm thick and 0.33 kg heavy; the second one is 40 mm thick and 0.44 kg heavy. The two oscillators are carved from single aluminum blocks, whose external parts are kept together by INVAR spacers and represent the external frames of the structure (see Fig. 1). Two rows of 12.7 mm diameter mirrors form the FFP: five on one mass, including a flat, 130 ppm transmission input mirror and a 1 m radius end mirror angled by 18°, and four flat mirrors on the opposite mass. The distance between opposite mirror surfaces is $D = 20$ mm. The input mirror is positioned on the outer side of the 30 mm thick mass with respect to the other mirrors of the row, for easier alignment. The FFP cavity length is $L = 200$ mm. Because of the non-normal reflections, for each longitudinal mode the *s*-polarization resonance frequency is detuned by 6 MHz from the *p*-polarization resonance (the mirror coating is optimized for normal incidence), with no appreciable linewidth difference. The prototype is placed on a cantilever mechanical suspension in a thermally stabilized vacuum chamber.

The mechanical properties of the two coupled oscillators have been characterized by positioning accelerometers on the two frames and analyzing the response to a global mechanical excitation. A comparison with a Finite Element Method (FEM) model allows us to identify the peaks corresponding to the translation and torsion modes of the two masses (their shapes are shown in Fig. 4. In particular, the translation modes are found at ~800 Hz (for the heavier mass) and ~1200 Hz (for the lighter mass). The same FEM analysis gives the effective masses of the translation modes, excited and read on a small circular area corresponding to the central mirrors. The results are, respectively, 0.31 kg and 0.41 kg, not far from the physical masses.

The experimental setup for the opto-mechanical characterization of the prototype is sketched in Fig. 2. The light source is a cw Nd:YAG laser working at 1064 nm. After a 40 dB optical isolator, the laser radiation is split into two

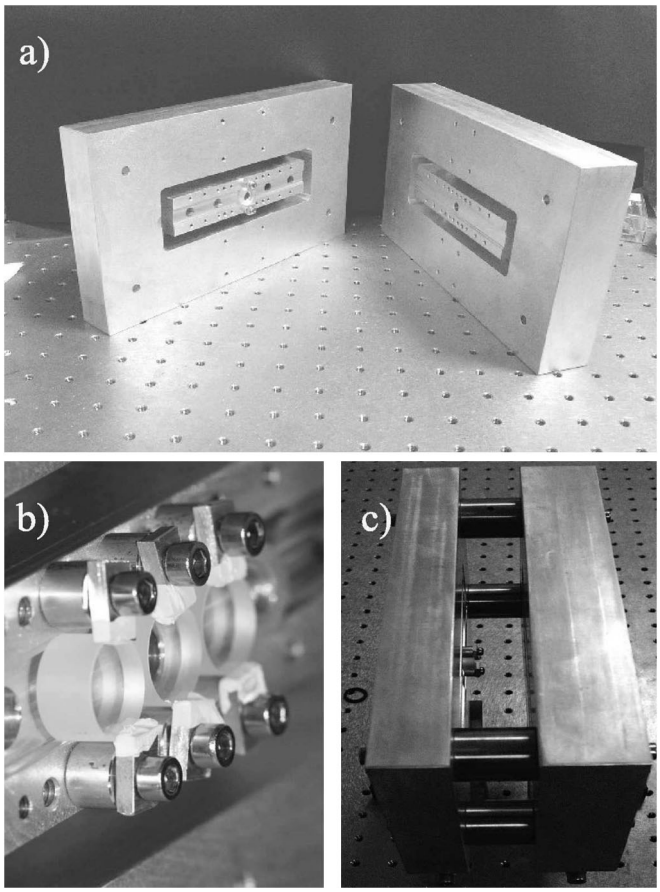

FIG. 1. Photos of our prototype double oscillator with folded Fabry-Perot readout. (a) The two frames, with the oscillating masses in the center; the masses are connected to the frames by leaving lateral membranes on the back of the frames. (b) Three mirrors of a row of five are fixed on one mass (in Figs. a) and (c) one mirror is left as reference). (c) The device is assembled with INVAR spacers.

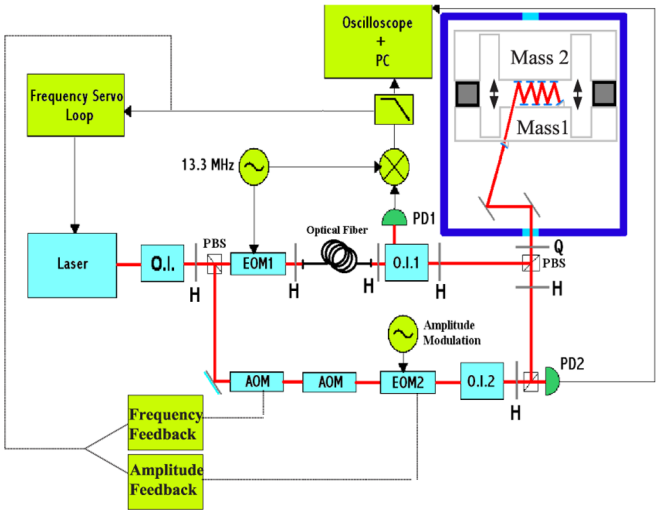

FIG. 2 (color online). Scheme of the experimental apparatus. O.I.: optical isolator; AOM: acousto-optic modulator; EOM: electro-optic modulator; H: half-wave plate; Q: quarter-wave plate; PD: photodiode; PBS: polarizing beam splitter. The double arrows indicate the translation motion of the test masses. The servo loops shown with dashed lines are only used in the cooling experiment, alternatively in the two configurations (with feedback acting in the frequency or in the amplitude of the cooling beam).

beams. On the first one, a resonant electro-optic modulator (EOM1) provides phase modulation at 13.3 MHz with a depth of about 1 rad used for the Pound-Drever-Hall [23] (PDH) detection scheme. The light is then transmitted by a polarization maintaining optical fiber and a second optical isolator (O.I.1). The second beam can be shifted in frequency by means of two acousto-optic modulators (AOM) and modulated in amplitude by an EOM (EOM2) followed by an optical isolator (O.I.2). We use, respectively, the $+1$ and -1 diffracted orders of the AOMs, so that the total frequency displacement corresponds to the difference of the AOM frequencies and can be tuned by several MHz around zero. After O.I.2, part of the second beam is detected by a photodiode (PD2) for monitoring its amplitude modulation. The two beams are combined with orthogonal polarizations in a polarizing beam-splitter and sent to the folded optical cavity. A quarter-wave plate allows us to optimize the matching of the polarization to the cavity modes. The reflected first beam, on his back path, is deviated by the input polarizer of the O.I.1 and collected by a photodiode (PD1) for the PDH detection. This PDH signal is used for laser frequency locking, while the second beam is tuned across the resonance using the AOMs. Even when both beams are resonant with respect to the respective polarization modes, their frequency splitting allows to eliminate any spurious interference and cross talk.

The displacement noise spectrum has been obtained directly from the Pound-Drever signal with the laser weakly locked on the cavity, and stopping the second beam. The signal is calibrated by modulating the laser frequency through its internal piezoelectric crystal, with a depth and a modulation frequency smaller than the FFP cavity linewidth, and using a phase-sensitive detection on the PDH signal. The laser piezoelectric crystal is itself calibrated by observing the sidebands at 13.3 MHz on a wide, slow enough scan. The PDH calibration procedure, performed varying the modulation frequency, allows also to correct the data for the servo loop.

In order to characterize the response of the FFP to variations of the intracavity power, the laser is weakly locked on the cavity using the first beam while the second beam is amplitude modulated at different frequencies. The extraction of the cavity response is obtained again from the PDH signal. The signal from PD2 and PD1 are acquired simultaneously with a digital oscilloscope, and successively elaborated to infer the component synchronous with the modulation. The depth of the intracavity power modulation is calculated from the signal of PD2 by taking

into account the mode matching and the cavity coupling factor. The latter is inferred from the depth of the dip in the reflected beam when scanning on the resonance, and it is consistent with the independent measurements of cavity Finesse and input mirror transmission.

A first important test concerns the optical properties of the FFP configuration, that had not been implemented before. We could indeed obtain a mode matching of 93% (comparable with that obtained with a simple cavity) and a Finesse of 6000 (linewidth 125 kHz) with an intracavity optical power of the order of 1 W, in agreement with a calculation based on the independently measured losses of the mirrors.

III. OPTO-MECHANICAL CHARACTERIZATION

A. Displacement noise spectrum

The cavity length noise spectrum evidences the mechanical modes directly coupled to the optical cavity (i.e., modes changing the intracavity optical path). Among them, it is possible to recognize the lower order translation and torsion modes, previously identified in the mechanical characterization of the cavity (Fig. 4). These mechanical resonances emerge from a background given by the free-running laser frequency noise (in the frequency region of interest, it is approximately $10^8/f^2$ Hz^2/Hz where f is the frequency expressed in Hz).

The vertical scale in Fig. 4 is expressed in terms of spectral density of variations δL of the cavity optical length L (measured from the input mirror to the end mirror), which are directly inferred from the measured spectrum using the calibration procedure described in the previous section. For an intuitive understanding, the system can be approximated by infinitely rigid masses linked with massless membranes to a still frame. With this scheme, the translation modes corresponds to pure translations of the masses on the cavity plane and perpendicularly to the mirror surfaces, as shown by arrows in Fig. 2. In this case, simple geometrical considerations (illustrated in Fig. 3) lead to the relation

$$\delta L = 8\cos\theta\,\delta D, \tag{1}$$

where δD is the (small) variation of the distance between the two masses, δL is the corresponding change in the cavity optical length, and θ is the incidence angle on the folding mirrors (18° in our case). The expression (1), inverted, can be used to convert the measured displacement from δL to δD. In this way, from the measurement in Fig. 4 we can directly deduce the displacement of 'ideal' translation modes, while for other mechanical modes one can only see in the spectrum the corresponding fluctuations of the cavity length. In the approximated scheme with rigid masses, the relevant torsion modes correspond to rotations of the mass around an horizontal (modes a, b in Fig. 4) or a vertical axis (mode d in the figure). In this approximation, such modes do not change the cavity length at the first order in the angular motion. Therefore, the system should be completely blind to the torsion modes, that are excited and detected only thanks to deformations in the masses and frames.

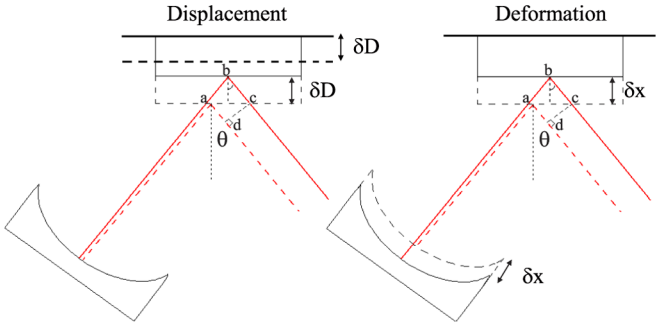

FIG. 3 (color online). Scheme of the optical length change in the case of a mass displacement δD (left) or a photo-thermal deformation δx (right). In the case of the folding mirror, the path change is (considering the right panel) $(ad - abc) = 2\cos\theta\,\delta x$, while for the end mirror it is simply δx. The incidence angle (18° in our setup) is exaggerated for clearness.

The mechanical quality factors of the modes, measured from their spectral width, are, respectively, 1800 (heavy mass translation mode at 795 Hz), 850 (light mass translation mode at 1190 Hz), and 310 (heavy mass torsion mode around a vertical axis, at 1166 Hz).

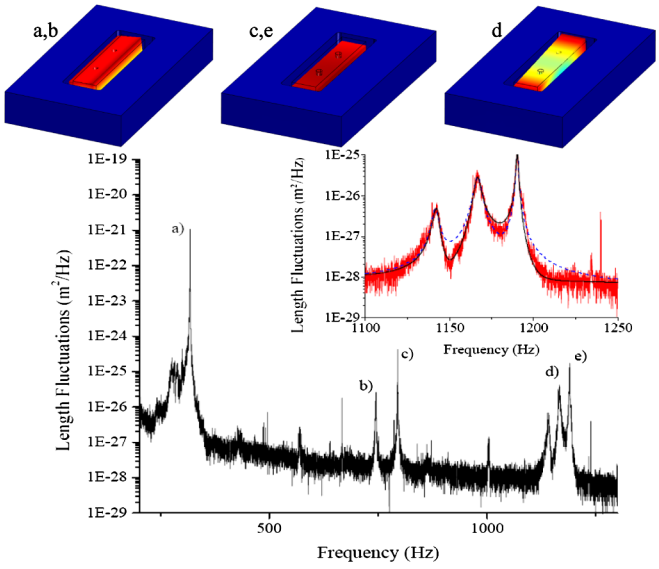

FIG. 4 (color online). Spectral density of the cavity length fluctuations. Some of the peaks are attributed to particular modes by comparison with the FEM model, namely, translation modes (c and e) and torsion modes (a, b, and d). Their structure is shown in the upper part of figure. For the translation modes, it is meaningful to attribute the signal to fluctuations in the distance D between the two masses, according to Eq. (1). In this way, the spectral density shown in the graph is reduced by a factor of $64\cos^2\theta \simeq 58$. In the inset, fit with thermal noise as in Eq. (3) (dashed line) and external noise as in Eq. (4) (solid line).

The ratio between the areas of the two peaks corresponding to the first order translation mode of the two masses is 1.45, in fair agreement with the value of 1.69 calculated by assuming a white driving force noise. A modal effective temperature $T_{\rm eff}$ can be calculated from these areas, according to

$$\int S_x \mathrm{d}\nu = \frac{kT_{\rm eff}}{M\omega_0^2}, \tag{2}$$

where S_x is the displacement noise spectral density, k is the Boltzmann constant, M is the modal mass and $\omega_0/2\pi$ its eigenfrequency. Using the values for the mass calculated by the FEM analysis, we obtain for the two modes effective temperatures of about 3300 K and 3900 K,, respectively, clearly showing that the effects of external, technical noise is about 1 order of magnitude larger than thermal noise. We can infer from this measurement an horizontal displacement noise, at the level of the FFP frames, of about $2 \cdot 10^{-33}$ m^2/Hz. This is compatible with seismic noise around 1 kHz, filtered by the optical table and the FFP suspension.

The excess external noise is also confirmed by the spectral shape around 1.2 kHz, where we find three nearly-degenerate modes: as already mentioned the highest frequency ($\sim$ 1190 Hz) belongs to the translation mode of the light mass, the intermediate frequency ($\sim$ 1166 Hz) is a torsion mode of the heavy mass, while the lowest frequency mode (around $\sim$1142 Hz) remains unidentified. In the case of thermal noise excitation, the contributions of all these modes should add incoherently in the noise spectrum, that should read [24,25]:

$$S_x = \frac{4kT}{\omega}\sum_i \mathrm{Im}\chi_i = 4kT\sum_i \frac{\omega_i}{Q_i M_i[(\omega_i^2-\omega^2)^2 + (\frac{\omega\omega_i}{Q_i})^2]}, \tag{3}$$

where for each mode χ_i is the susceptibility, M_i the mass, ω_i the eigenfrequency and Q_i the quality factor, and T is the thermodynamic temperature. On the other hand, an external noise $S_x^{\rm ext}$ should excite them coherently, and therefore be filtered by a superposition of modes response functions, such as:

$$S_x = \left|\sum_i \chi_i\right|^2 S_x^{\rm ext} = \left|\sum_i \frac{1}{M_i[\omega_i^2 - \omega^2 - i\frac{\omega\omega_i}{Q_i}]}\right|^2 S_x^{\rm ext}, \tag{4}$$

where the effective masses do not necessarily correspond to the previous ones.

We have fitted the experimental spectrum, in the mentioned region around 1.2 kHz, with the expressions (3) and (4). We remark that the two fitting procedures uses the same number of free parameters, namely, the set $\{Q_i, \omega_i\}_{i=1,3}$, three amplitudes, and the coefficient of the frequency noise background. Concerning the amplitude, we have chosen to fix the mass of the translation mode at its FEM value, leaving the other two masses as free and multiplying by an overall factor that can be identified with $S_x^{\rm ext}$ of expression (4) or with the temperature in expression (3). The two fitting curves are reported in the inset of Fig. 4. The fit with expression (4) is clearly better. A quantitative evaluation, underlining the contribution of the wings of the peaks where the difference between the two fitting functions is more evident, is obtained by calculating the quadratic sum of differences between the logarithm of the experimental data and of the corresponding theoretical values (in other words, the χ^2 in logarithmic scale). This indicator is a factor of 1.7 higher when using expression (3), with respect to Eq. (4). Since the number of free parameters is the same, the analysis gives a strong indication in favor of the model behind Eq. (4), with a flat external noise spectrum. Of course, this is confirmed by the unrealistically high temperature (or low mass) that would be required by expression (3). However, we remark here that, in the case of multiple overlapping peaks, there is not merely an increased spectral power due to extra-noise, but also a change in the shape of the spectrum that can be a stronger, calibration-independent indication.

B. Response to modulation of the intracavity power

In Fig. 5 we report the phase and amplitude response of the FFP to a modulation of the intracavity radiation intensity. The measured signal is reported in terms of changes in

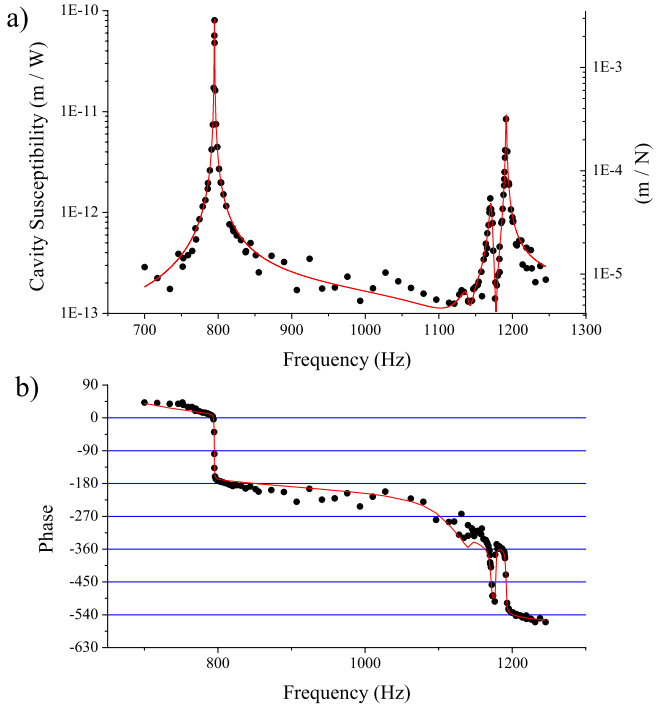

FIG. 5 (color online). Amplitude (upper graph) and phase (lower graph) of the response of the cavity length to modulation of intracavity power. The solid line is the result of a fitting procedure based on the expression (5).

the cavity length L. To obtain the response, the signal is divided by the amplitude of the modulation in the intracavity radiation pressure, giving a susceptibility in m/N.

Following the discussion in the previous section, the derived quantity has an intuitive interpretation only for the 'ideal' translation modes of the test masses. In this case, the relation (1) allows to find the variations of the mass positions and, as we will see later, to extract values of the modal masses directly comparable with the FEM model and/or the physical masses.

The mechanical resonances emerge on top of a (nearly) constant background associated with photo-thermal effect, i.e., to mirrors thermal expansion due to heating by the absorbed intracavity radiation [26,27]. This effect is more meaningfully expressed in terms of m/W, as indicated on the left vertical axis of Fig. 5. As will be discussed later in this section the quantitative explanation of the photo-thermal background implies the verification of the 'wide area readout' effect.

The complete response, between 700 Hz and 1250 Hz, is fitted to the coherent superposition of a constant, complex background C_{phth} and four mechanical resonance, using the following function:

$$X(\omega) = \sum_{i=1,4} \frac{A}{M_i[\omega_i^2 - \omega^2 - i\frac{\omega\omega_i}{Q_i}]} + C_{phth}. \qquad (5)$$

The fitting procedure considers at the same time both quadratures of the response, minimizing their distance, respectively, from ReX and ImX. The function obtained, expressed as amplitude and phase, is reported in Fig. 5 and the fitting parameters are summarized in Table I. The factor A is fixed to $32\cos^2\theta$; as we will show later (in Eq. (7) and the following discussion), this coefficient allows to attribute the modal masses M_i to vibrations of the test masses, excited and read on the laser spots.

For the translation modes (at 795 Hz and 1190 Hz) we infer effective masses of 0.2 kg and 0.34 kg, respectively.

TABLE I. Parameters obtained by fitting the experimental response to a modulated intracavity power with expression (5).

M_1 (Kg)	0.20
M_2 (Kg)	0.34
M_3 (Kg)	1.07
M_4 (Kg)	4.4
ν_1 (KHz)	0.795
ν_0 (KHz)	1.191
ν_0 (KHz)	1.171
ν_0 (KHz)	1.140
Q_1	1940
Q_2	835
Q_3	370
Q_3	70
$\lvert C_{phth}\rvert$ (m/W)	1.34×10^{-13}
Phase (C_{phth}) (0)	23

While for the latter the agreement with the physical mass and FEM simulation is good, for the former it is only marginal. The effective mass of the torsion mode at 1166 Hz is about 1 kg, much more than the physical mass involved in the motion, showing that, as expected, the readout is nearly blind to this mode. Also this effect is particularly important for DUAL, where the readout topology is studied in order to minimize the effect of disturbing mechanical modes within the useful detection band [5].

Concerning the mechanical quality factors, the values obtained from the fit are, respectively, 1940 (at 795 Hz), 835 (at 1191 Hz), and 370 (at 1171 Hz), all in good agreement with the corresponding figures given by the displacement noise spectrum. The fourth resonance (around 1140 Hz) is barely visible.

It is particularly interesting the region around 1.2 kHz, shown in detail in Fig. 6, where a torsion and a translation mode are very close. Here, between the two peaks, the complete response falls below each single peak contribution (shown with dashed lines in the figure), due to their interference. This effect implies a cancellation of the back-action: the system is less sensitive to modulation of the intracavity power, and therefore also to laser amplitude fluctuations and radiation shot-noise, which are the physical origin of the back-action. On the other hand, the effect of a force acting on both modes in the same direction would be amplified. The same should happen between the two gw sensitive modes of a DUAL detector. The demonstration of this effect on our prototype would be even clearer by exploiting the translation modes of the two masses, for which the reaction to a gw is more intuitive, but it is prevented by the photo-thermal background.

Let us now consider the other crucial issue of DUAL: the 'wide area readout'. In the case of optical readout, it can be implemented by the multispot configuration of the FFP. We first summarize its working principle, in the simple scheme of N spots on one surface and $N + 1$ on the opposite one.

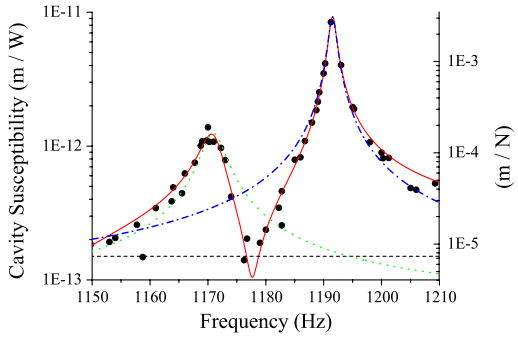

FIG. 6 (color online). Enlargement of the response shown in Fig. 5, together with a complete fitting function (red, solid line), the contributions of two peaks (respectively green dotted and blue dashed-dotted lines) and contribution of the photo-thermal background (gray dashed line).

We suppose that the spots are far enough to neglect the overlap between local deformations, and the beam impinges with small incidence angle (more detailed studies are reported in Ref. [9]). In this case, if the first surface moves by δD, the change in the optical path is $\delta L = 2N\delta D$, with an increase by a factor of $2N$ with respect to a simple cavity. The radiation-pressure noise, due to intracavity power fluctuations, acts at the same time on all the spots. The resulting displacement noise power in the optical path is $S^L_{rp} = 4N^2 S^x_{rp}$, where S^x_{rp} are the fluctuations in the position of a single spot. It seems that the signal-to-noise remains unchanged with respect to a simple cavity, with both noise and signal power multiplied by $4N^2$. However, we must consider that in a FFP the intracavity power is reduced, and therefore also its fluctuations. Indeed, the intracavity power is $P_c = \frac{T}{(T+A_{\rm tot})^2} P_{\rm in}$ where T is the input mirror transmission, $A_{\rm tot}$ the other round-trip losses, $P_{\rm in}$ the input power. For an optimally coupled cavity (the best configuration for a PDH detection), with $T = A_{\rm tot}$, one has $P_c = P_{\rm in}/4A_{\rm tot}$. Now, in a FFP, $A_{\rm tot} = 2NA_{\rm single}$ where $A_{\rm single}$ are the losses in a single spot (in the round-trip, each spot is touched twice). Therefore the intracavity power is reduced by a factor of $2N$ and its power fluctuations by $4N^2$, as well as S^x_{rp}. As a consequence, the signal-to-noise power ratio is improved by a factor $4N^2$.

The calculation of the Brownian thermal noise is even simpler: we have uncorrelated noise fluctuations in the different spots, therefore $S^L_{th} = 4NS^x_{th}$ (S^L_{th} are the fluctuations in the FFP optical path, S^x_{th} the displacement thermal noise in a single spot) and the signal-to-noise is improved by a factor of N.

In this work the sensitivity is not enough to see the effects of 'local' thermal noise and radiation-pressure effects: the former is overwhelmed by laser frequency noise, the latter by photo-thermal background. However, for what the 'wide area readout' is concerned, such photo-thermal expansion behaves exactly like a deformation due to radiation pressure: phase and amplitude of the response are different, but the effects on the different spots sum up in the same way.

As a further difference with respect to the described model, we cannot optimize the input mirror transmission. However, we can measure the ratio between mechanical modes peaks and photo-thermal background in the response to modulated intracavity power. Thanks to the broad area readout, the peaks emerge from background stronger than in the case of a simple cavity. In particular, for our configuration, if $\delta x = \chi_{phth}\delta P_c$ is the photo-thermal displacement of each single spot due to a change δP_c in the intracavity power, the change in the FFP optical length is

$$\delta L^{FFP}_{phth} = 2(1 + 7\cos\theta)\chi_{phth}\delta P_c. \tag{6}$$

This is illustrated in Fig. 3: on the end mirrors the change of optical length is δx, while on the seven folding mirrors it is $2\cos\theta\delta x$. In the case of a simple cavity, summing the effects on its two mirrors, we would have $\delta L^{\rm simple}_{phth} = 2\chi_{phth}\delta P_c$.

Because of a translation mode of one FFP mass, with susceptibility at resonance χ_0, we have instead

$$\delta L^{FFP}_{\rm mode} = \frac{2}{c}(32\cos^2\theta)\chi_0\delta P_c, \tag{7}$$

to be compared with the simple cavity expression

$$\delta L^{\rm simple}_{\rm mode} = \frac{2}{c}\chi_0\delta P_c. \tag{8}$$

Equation (7) is obtained by using Eq. (1) and the mass displacement $\delta D = \chi_0\delta F$ where $\delta F = 4(\frac{2}{c}\cos\theta\delta P_c)$ due to the four bounces. We finally derive

$$\frac{\delta L^{FFP}_{\rm mode}}{\delta L^{FFP}_{phth}} = \frac{2}{c}\frac{32\cos^2\theta}{2(1+7\cos\theta)}\frac{\chi_0}{\chi_{phth}} \tag{9}$$

for the FFP, and

$$\frac{\delta L^{\rm simple}_{\rm mode}}{\delta L^{\rm simple}_{phth}} = \frac{2}{c}\frac{\chi_0}{2\chi_{phth}} \tag{10}$$

for a simple cavity.

We have measured the photo-thermal expansion in a simple Fabry-Perot cavity with the same mirrors used in the FFP and roughly the same beam size (the cavity length is 0.2 m) [22]. In the frequency range of interest (around 1 kHz) the effect has a weak dependence on the frequency, and for each single mirror is $|\chi_{phth}| = 10^{-14}$ m/W. Using this value in the expression (6), we infer $\delta L^{FFP}_{phth}/\delta P_c \simeq 1.5 \cdot 10^{-13}$ m/W, in good agreement with the value of 1.3×10^{-13} m/W obtained from the fit of the experimental data (reported with a dashed line in Fig. 6).

Concerning the peak-to-background ratio, taking for instance the first translation mode at 800 Hz with $\chi_0 = 3.9 \cdot 10^{-4}$ m/N, we calculate $\delta L^{FFP}_{\rm mode}/\delta L^{FFP}_{phth} = 520$ and $\delta L^{\rm simple}_{\rm mode}/\delta L^{\rm simple}_{phth} = 130$, to be compared with the experimental value of 540.

The data presented here can be considered as the first experimental verification of the 'wide area readout' effect, for the particular case of multispot readout.

IV. RADIATION PRESSURE COOLING

The experimental scheme for the radiation pressure cooling of a FFP translation mode is similar to the setup implemented for the measurement of the response to modulated intracavity power. The measurement beam is weakly locked to a resonance of the optical cavity, and its PDH signal is used also for obtaining the spectrum of the cavity length fluctuations. The calibration of the spectral measurement is performed with the procedure described in Sec. II, even if now we are just interested in a narrow frequency region around the peak at ~800 Hz. The same

PDH signal, amplified and integrated, is used as correction signal acting on the second beam for the active radiation-pressure cooling.

We have experimented two different cooling schemes. In the first case, the second beam is tuned on resonance of its polarization mode, and we act on its intensity (by means of EOM2). This configuration implements a standard optical 'cold damping', like the one firstly demonstrated in Ref. [12] and later, i.e., in Ref. [13]. With respect to the mentioned works, here we have a close spatial matching between sensing and cooling beams.

In the second scheme, the cooling beam is frequency shifted on the average by half linewidth from resonance, and the feedback acts on the beam detuning (by means of one AOM) which actually controls the intracavity power. This configuration is somehow original: its working principle is the same as in Ref. [18] (the so-called hybrid scheme), with the difference that here we react on the laser-to-cavity detuning by changing the laser frequency instead of the cavity length. An important characteristics that distinguishes our experiment from the those described in Refs. [18,19] is the use of two separate laser beams for measuring the mass motion and for cooling. In this way, the measured signal (i.e., the detuning between the probe beam and the cavity) is not directly modified by the cooling servo loop, that only acts on the frequency of the second beam without directly modifying the probe frequency, nor the cavity length. This procedure eliminate the necessity to correct the acquired data for the feedback: the probe beam can be considered as free-running and the PDH signal gives directly the cavity length fluctuations, thus allowing a clearer interpretation of the results.

The physics behind active cooling is described in Refs. [11,12] and in several subsequent articles. We summarize here its main features, also in order to clarify our experiment.

In general, a signal proportional to the detuning is frequency filtered and transformed into a force acting on the oscillator. The evolution equation of the oscillator position, in the Fourier space, reads

$$M\left(\omega_0^2 - \omega^2 - i\frac{\omega\omega_0}{Q}\right)\tilde{x} = \tilde{f}_{th} + G\tilde{x}, \tag{11}$$

where G is a general complex, frequency-dependent gain function and $\tilde{f}_{th}$ is the noise force, that in the case of Brownian thermal noise has spectral density [24]

$$S_{th} = \frac{4kTM\omega_0}{Q}. \tag{12}$$

A general, white force noise can be included by replacing the thermodynamic temperature T with a noise temperature. Equation (11) gives

$$\tilde{x} = \frac{\tilde{f}_{th}}{M(\omega_{\rm eff}^2 - \omega^2 - i\frac{\omega\omega_{\rm eff}}{Q_{\rm eff}})} \tag{13}$$

with $\omega_{\rm eff}^2 = \omega_0^2 - {\rm Re}G/M$ and $\frac{\omega_{\rm eff}}{Q_{\rm eff}} = \frac{\omega_0}{Q} + \frac{{\rm Im}G}{M\omega}$.

Taking a feedback proportional to the oscillator velocity, e.g., $G = -igM\omega\omega_0$, the effective eigenfrequency and quality factor do not depend on ω, and the equation of motion is the same as the one of a free oscillator, with modified damping ($1/Q_{\rm eff} = 1/Q - g$) and temperature. In particular, for $g > 0$ the quality factor is increased and the effective temperature, obtained from the integral of the spectrum as in Eq. (15), is increased as $T_{\rm eff} = TQ_{\rm eff}/Q = T/(1 - Qg)$. The same expressions for negative g gives lowering quality factor and temperature ('cold damping').

If G has a different dependence on ω, the parallelism between the modified evolution equation and a free oscillator is not straightforward. Even in simple realistic schemes the energy equipartition does not hold and a system temperature is not well defined, as discussed, e.g., in Ref. [28]. However, for high quality factor, most of the fluctuations are localized in a narrow spectral region around resonance and we can use a Lorentzian approximation of the spectrum, so that

$$S_x \simeq \frac{S_{th}}{M^2\omega_{\rm eff}^2[4(\omega_{\rm eff} - \omega)^2 + (\frac{\omega_{\rm eff}}{Q_{\rm eff}})^2]}, \tag{14}$$

where in $\omega_{\rm eff}$ and $Q_{\rm eff}$ we can replace $G(\omega)$ by its value at ω_0. Even a colored external noise can be included in the discussion, provided that it has a smooth spectrum in the region of the peak. In this case an effective temperature can still be defined according to Eq. (15), that gives

$$T_{\rm eff} = \frac{T}{1 + Q\frac{{\rm Im}G(\omega_0)}{M\omega_0^2}}, \tag{15}$$

while the effective eigenfrequency is shifted by the real part of the gain.

In the adiabatic limit, for frequencies well below the cavity linewidth, the force exerted by radiation pressure can be written as

$$F_{rp} = \frac{2}{c}\frac{P_c}{1 + \Delta^2}, \tag{16}$$

where P_c is the intracavity power at resonance and Δ the detuning normalized to the cavity half-linewidth γ.

In the standard 'cold damping' scheme, the laser is kept at resonance and a signal proportional to the detuning is sent to correct the laser power. Neglecting the laser frequency fluctuations and the cavity length noise (except for the oscillating mirror position x), the loop gain can be written as

$$G = \frac{2}{c}P_c G_{el}, \tag{17}$$

where G_{el} is a (complex and frequency-dependent) elec-

tronic servo loop gain expressed as the ratio between the detuning fluctuations $\tilde{x}$ and the consequent imposed relative power fluctuations.

In the hybrid configuration, the cooling laser is detuned and the feedback is on the detuning. We can expand Eq. (16) around the working point Δ_0, obtaining for the radiation-pressure force fluctuations $\tilde{f}_{rp}$

$$\tilde{f}_{rp} = -\frac{2}{c} P_c \frac{2\Delta_0}{(1+\Delta_0)^2} \frac{1}{\gamma}\left(\tilde{x} + \tilde{l} + \frac{l_{\rm cav}}{\nu_L}\tilde{\nu}_L\right) \tag{18}$$

where $l_{\rm cav}$ is the average cavity length, $\tilde{l}$ its fluctuations, ν_L is the cooling laser frequency with fluctuations $\tilde{\nu}_L$, and we have neglected laser amplitude noise. The cavity and/or the laser frequency fluctuations may contain a term proportional to $\tilde{x}$ through electronic servo loop gains that we call respectively G_l and $(l_{\rm cav}/\nu_L)G_\nu$. This term is obtained from a measurement of the detuning between the cavity and a probe beam. Equation (18) can now be written in an interesting form as

$$\tilde{f}_{rp} = -K_{os}[(1 + G_l + G_\nu)\tilde{x} + \tilde{n}], \tag{19}$$

where

$$K_{os} = \frac{4P_c\Delta_0}{\gamma c(1+\Delta_0)^2} \tag{20}$$

is the optical spring rigidity [29] and $\tilde{n}$ is a general extra-noise term. The meaning of K_{os} is clear when replacing Eq. (19) in the expression for $\omega_{\rm eff}$: the effect of radiation pressure is modifying the oscillator spring rigidity $(M\omega_0^2)$ according to $M\omega_{\rm eff}^2 = {\rm Re}K_{os} + M\omega_0^2$. An oscillator damping is imposed by the reactive component of the optical spring. In the passive 'self-cooling' it is given by the delay in the optical field buildup inside the cavity (that we have neglected in the adiabatic approximation). In the active scheme, it is obtained by the feedback that, as we see in Eq. (19), 'modifies' the optical spring rigidity.

Concerning the extra-noise, it includes (a) the cavity length noise $\tilde{l}^n$ entering both directly in $\tilde{l}$ and from the measurement exploited for cooling (i.e., through the servo-loop); (b) the cooling laser frequency noise $\tilde{\nu}_L^n$; (c) the probe beam frequency noise $\tilde{\nu}_{\rm probe}$. We have therefore

$$\tilde{n} = \tilde{l}^n(1 + G_l + G_\nu) + \frac{l_{\rm cav}}{\nu_L}[\tilde{\nu}_L^n + (G_l + G_\nu)\tilde{\nu}_{\rm probe}]. \tag{21}$$

The right-end side of Eq. (11) becomes $\tilde{f}_{th} - K_{os}(1 + G_l + G_\nu)\tilde{x} - K_{os}\tilde{n}$ and we are in the conditions of the previous general discussion by replacing $-K_{os}(1 + G_l + G_\nu) \rightarrow G$ and adding to the force noise spectrum S_{th} the additional term $K_{os}^2 S_n$, where S_n is the spectral density of $\tilde{n}$.

In our case, the dominant term in S_n comes from the probe beam frequency noise S_ν and the feedback on the cooling beam frequency is characterized by $|G_\nu| \gg 1$. Therefore, we can write $S_n \simeq (l_{\rm cav}/\nu_L)^2|G|^2 S_\nu$ and, expressing the gain as $G = |G|\exp(i\phi)$, the equation for the effective temperature given in Eq. (15) can be written in the useful form

$$\frac{T_{\rm eff}}{T} = \frac{1 + a(\frac{P_{\rm in}}{P_0})^2}{1 + \frac{P_{\rm in}}{P_0}}, \tag{22}$$

where $P_{\rm in}$ is the input power of the cooling beam, the normalization constant P_0 is

$$P_0 = \frac{\gamma c(1+\Delta_0)^2}{4\Delta_0}\frac{M\omega_0^2}{Q}\frac{P_{\rm in}}{P_c} \tag{23}$$

and the extra-noise coefficient a is

$$a = \frac{l_{\rm cav}^2}{\nu_L^2}\frac{S_\nu}{S_x(0)}\frac{1}{\sin^2\phi}, \tag{24}$$

where $S_x(0) = S_{th}Q^2/(M^2\omega_0^4)$ is the displacement noise at resonance measured before cooling. We remark that, for the optimal feedback phase $\phi = \pi/2$, the value of a can be inferred directly from the displacement noise spectrum: $S_x(0)$ is the peak value, and $l_{\rm cav}^2 S_\nu/\nu_L^2$ is the background. The minimum effective temperature $T_{\rm min}$, achievable for $P_{\rm in}/P_0 = \sqrt{1 + 1/a} - 1$, is $T_{\rm min}/T = 2a(\sqrt{1 + 1/a} - 1) \simeq 2\sqrt{a}$.

We could achieve cooling of the translation mode both with 'cold damping' and with the hybrid scheme. An example of the displacement noise spectra modified by cooling is reported in Fig. 7 for the second configuration (with frequency feedback on the cooling beam). Here we focus on the translation mode of the heavy mass, around 800 Hz, and we have transformed the cavity length fluctu-

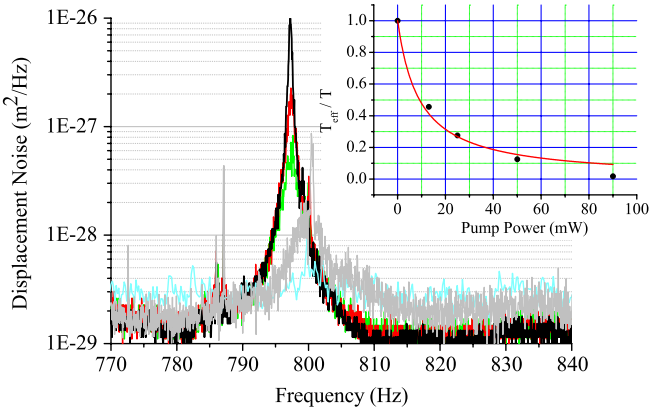

FIG. 7 (color online). Spectral measurement of the heavy mass displacement noise, around the resonance of its lower translation mode, for different values of the cooling laser power. From dark to light lines, the corresponding laser power values measured before the cavity are 0 (black line), 13 mW (red), 25 mW (green), 50 mW (light grey) and 90 mW (light blue). In the inset, the ratio between effective temperature $T_{\rm eff}$ and initial temperature T (symbols) as a function of the cooling laser power, fitted by Eq. (22) (red line).

ations into mass position fluctuations using the relation (1). The effective temperature of the mode, estimated from the area of the spectral peak, is reduced by a factor of more than 10, as shown in the inset of the figure. The cooling factor is limited the laser frequency noise and, with strong cooling power, the peak of the mechanical resonance disappears completely in the frequency noise background. The measured effective temperature is fitted by Eq. (22) fixing the extra-noise factor a at the value of $1.1 \cdot 10^{-3}$, measured form the spectrum shown in Fig. 4. For the highest cooling power level, a weak instability in the electronic feedback loop slightly enhances the background noise. As a consequence, the uncertainty in the last temperature measurement is higher and we have not included in the fit, that gives $P_0 = 9.7$ mW and therefore a best obtainable cooling of $T_{\mathrm{min}}/T = 0.064$ for $P_{\mathrm{in}} = 280$ mW.

V. CONCLUSIONS

We have presented an experiment aimed at demonstrating and testing the main new concepts on which are based the proposals of DUAL gravitational wave detector. In particular, we show the 'backaction reduction' and the 'wide area readout' effects. Our prototype also contains the first implementation of Folded Fabry-Perot cavity, an optical scheme particularly conceived for DUAL.

We report a complete characterization of the mechanical response of ~kg mass oscillators, performed by exciting the system with radiation-pressure force. Moreover, we describe active optical cooling of an oscillator mode, also exploiting an original scheme with feedback on the laser frequency. Such experiences scale up the mass by several orders of magnitude with respect to previous experiments on opto-mechanical effects, and focus on the ~kHz frequency region, of interest for large mass gravitational wave detectors. Therefore, they represent a significant step for realistic planning of the next generation of massive detectors, whose possible optical readout should be pushed to the quantum regime where radiation-pressure effects are critical [8].

ACKNOWLEDGMENTS

This work was partially funded by the European Union ILIAS Project (No. RII3-CT-2003-506222). We thank M. Cerdonio and M. De Rosa for useful discussions.

[1] M. Cerdonio, L. Conti, J. A. Lobo, A. Ortolan, L. Taffarello, and J. P. Zendri, Phys. Rev. Lett. **87**, 031101 (2001).
[2] T. Briant *et al.*, Phys. Rev. D **67**, 102005 (2003).
[3] M. Bonaldi, M. Cerdonio, L. Conti, M. Pinard, G. A. Prodi, L. Taffarello, and J. P. Zendri, Phys. Rev. D **68**, 102004 (2003).
[4] T. Caniard, P. Verlot, T. Briant, P. F. Cohadon, and A. Heidmann, Phys. Rev. Lett. **99**, 110801 (2007).
[5] M. Bonaldi *et al.*, Phys. Rev. D **74**, 022003 (2006).
[6] F. Marin, Proceedings of the GWADW, Elba, Italy, 2006.
[7] C. M. Caves, Phys. Rev. D **23**, 1693 (1981).
[8] J. Belfi and F. Marin, Phys. Rev. D **77**, 122002 (2008).
[9] F. Marin, L. Conti, and M. De Rosa, Phys. Lett. A **309**, 15 (2003); Classical Quantum Gravity **21**, S1237 (2004).
[10] D. Vitali, S. Mancini, L. Ribichini, and P. Tombesi, Phys. Rev. A **65**, 063803 (2002).
[11] S. Mancini, D. Vitali, and P. Tombesi, Phys. Rev. Lett. **80**, 688 (1998).
[12] P. F. Cohadon, A. Heidmann, and M. Pinard, Phys. Rev. Lett. **83**, 3174 (1999).
[13] D. Kleckner and D. Bouwmeester, Nature (London) **444**, 75 (2006).
[14] S. Gigan *et al.*, Nature (London) **444**, 67 (2006).
[15] O. Arcizet, P. F. Cohadon, T. Briant, M. Pinard, and A. Heidmann, Nature (London) **444**, 71 (2006).
[16] A. Schliesser, P. Del'Haye, N. Nooshi, K. J. Vahala, and T. J. Kippenberg, Phys. Rev. Lett. **97**, 243905 (2006).
[17] J. D. Thompson, B. M. Zwickl, A. M. Jayich, F. Marquardt, S. M. Girvin, and J. G. E. Harris, Nature (London) **452**, 72 (2008).
[18] C. M. Mow-Lowry, A. J. Mullavey, S. Goßler, M. B. Gray, and D. E. McClelland, Phys. Rev. Lett. **100**, 010801 (2008).
[19] T. Corbitt *et al.*, Phys. Rev. Lett. **98**, 150802 (2007); **99**, 160801 (2007).
[20] A. Vinante *et al.*, Phys. Rev. Lett. **101**, 033601 (2008).
[21] M. De Rosa, L. Conti, M. Cerdonio, M. Pinard, and F. Marin, Phys. Rev. Lett. **89**, 237402 (2002).
[22] M. De Rosa, F. Marin, F. Marino, O. Arcizet, A. Heidmann, and M. Pinard, Classical Quantum Gravity **23**, S259 (2006).
[23] R. W. P. Drever, J. L. Hall, F. V. Kowalski, J. Hough, G. M. Ford, A. J. Munley, and H. Ward, Appl. Phys. B **31**, 97 (1983).
[24] P. R. Saulson, Phys. Rev. D **42**, 2437 (1990).
[25] We use in this article singleside spectra.
[26] V. B. Braginsky, M. L. Gorodetsky, and S. P. Vyatchanin, Phys. Lett. A **264**, 1 (1999).
[27] M. Cerdonio, L. Conti, A. Heidmann, and M. Pinard, Phys. Rev. D **63**, 082003 (2001).
[28] C. Genes, D. Vitali, P. Tombesi, S. Gigan, and M. Aspelmeyer, Phys. Rev. A **77**, 033804 (2008).
[29] V. B. Braginsky, Y. I. Vorontsov, and F. Y. Khalili, Sov. Phys. JETP **46**, 705 (1977); V. B. Braginsky, M. L. Gorodetsky, and F. Y. Khalili, Phys. Lett. A **232**, 340 (1997).